

Molecular Design of a Chiral Brønsted Acid with Two Different Acidic Sites: Regio-, Diastereo-, and Enantioselective Hetero-Diels–Alder Reaction of Azopyridinecarboxylate with Amidodienes Catalyzed by Chiral Carboxylic Acid–Monophosphoric Acid

Norie Momiyama,^{*,†,‡} Hideaki Tabuse,[§] Hirofumi Noda,^{||} Masahiro Yamanaka,^{||} Takeshi Fujinami,[†] Katsunori Yamanishi,[†] Atsuto Izumiseki,^{†,‡} Kosuke Funayama,^{§,⊥} Fuyuki Egawa,[§] Shino Okada,[¶] Hiroaki Adachi,[¶] and Masahiro Terada^{*,§,#}

[†]Institute for Molecular Science, Okazaki, Aichi 444-8787, Japan

[‡]SOKENDAI (The Graduate University for Advanced Studies), Okazaki, Aichi 444-8787, Japan

[§]Department of Chemistry, Graduate School of Science, Tohoku University, Aoba-ku, Sendai 980-8578, Japan

^{||}Department of Chemistry, Faculty of Science, Rikkyo University, Toshima-ku, Tokyo, 171-8501, Japan

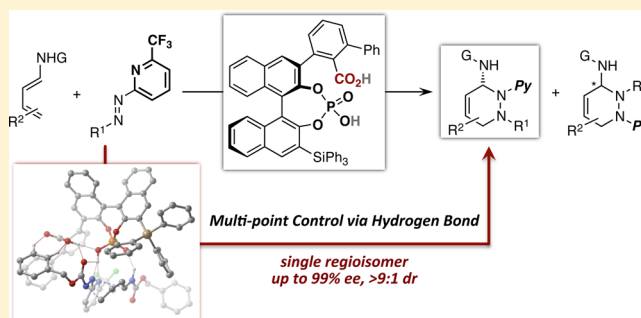
[⊥]Graduate Research on Cooperative Education Program of IMS with Tohoku University, Okazaki, Aichi 444-8787, Japan

[¶]SOSHO, Inc., 2-1 Yamadaoka, Suita, Osaka 565-0871, Japan

[#]Analytical Center for Giant Molecules, Graduate School of Science, Tohoku University, Aoba-ku, Sendai 980-8578, Japan

S Supporting Information

ABSTRACT: A chiral Brønsted acid containing two different acidic sites, chiral carboxylic acid–monophosphoric acid **1a**, was designed to be a new and effective concept in catalytic asymmetric hetero-Diels–Alder reactions of azopyridinecarboxylate with amidodienes. The multipoint hydrogen-bonding interactions among the carboxylic acid, monophosphoric acid, azopyridinecarboxylate, and amidodiene achieved high catalytic and chiral efficiency, producing substituted 1,2,3,6-tetrahydropyridazines with excellent stereo-control in a single step. This constitutes the first example of regio-, diastereo-, and enantioselective azo-hetero-Diels–Alder reactions by chiral Brønsted acid catalysis.



INTRODUCTION

Chiral Brønsted acid catalysis has recently been recognized as one of the fundamental tools in asymmetric synthesis.¹ A number of useful chiral Brønsted acids have been developed with appropriate acidic functional groups. Many such catalysts incorporate two of the same type of acidic functional groups, while others have one acidic site in a seven-membered ring structure, such as those in binaphthyl systems. Furthermore, combinations of these have effectively produced powerful chiral Brønsted acid catalysts.² In this context, we have been fascinated for some time with the development of hetero-combined Brønsted acid catalyst systems,³ with a particular focus on combinations of monophosphoric acids⁴ with other Brønsted acids.⁵ Despite having the potential for unprecedented catalytic activity because of a distinctive hydrogen-bond interaction using each acidic functional group, such a design concept remains poorly studied in the development of chiral Brønsted acid catalysts.

Encouraged by recent reports from our group,⁶ we became interested in hydrogen bond-mediated multipoint control⁷ with

two different acidic functional groups in catalytic asymmetric reactions. We report herein a chiral Brønsted acid catalyst with two different acidic sites, carboxylic acid–monophosphoric acid (Figure 1), designed specifically to elaborate the chiral environment using properly oriented multiple hydrogen bonds during catalysis. Describing primary interactions, an

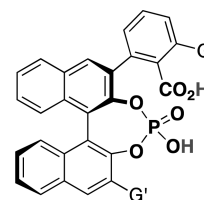


Figure 1. (R)-1,1'-Binaphthol-derived chiral carboxylic acid–monophosphoric acid.

Received: July 11, 2016

Published: August 16, 2016

intramolecular hydrogen bond between carboxylic acid and monophosphoric acid would allow the catalyst to establish a favorable diastereomeric structure for high stereoselectivities^{3c,d,6} (Figure 2). This intramolecular hydrogen bond design

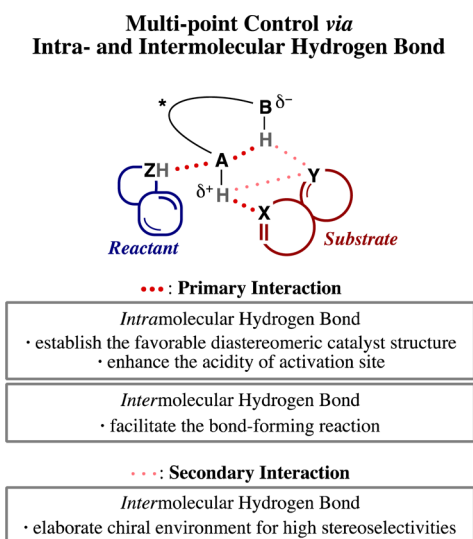


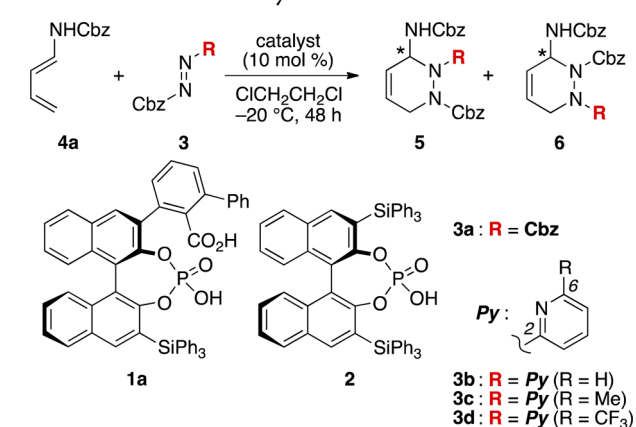
Figure 2. Design concept of a chiral Brønsted acid with two different acidic sites: Multipoint control by *intra*- and *intermolecular* hydrogen bond. AH/BH indicates either CO₂H/PO₃H or PO₃H/CO₂H. X/Y/Z indicates Lewis basic sites such as O, N, etc.

would not only regulate the diastereomeric catalyst structure but also result in the increased acidity of the catalyst, enabling catalytic activity that would be entirely unique when compared to chiral Brønsted acids with one acidic functional group. Intermolecular hydrogen bonds among the catalyst, the substrate, and the reactant are responsible for facilitating the bond-forming reaction. In addition, we envisioned that a secondary, weaker interaction would exist as an *intermolecular* hydrogen bond between the acidic functional groups and Lewis basic sites of the substrates, and this would contribute to the stereo- and regioselectivity of the reaction.

RESULTS AND DISCUSSION

1. Enantioselective Hetero-Diels–Alder Reaction of Azocarboxylates with *N*-H-Amidodienes. Enantioselective hetero-Diels–Alder reactions⁸ of azocarboxylates with *N*-H-amidodienes were selected as an initial probe to test the hypothesis that multiple hydrogen bonds will provide enhanced reactivity and selectivity in catalysis.^{9,10} Initial experiments used two types of azocarboxylates, **3a** and **3b**, as the hydrogen bond acceptors with the carboxylic acid–monophosphoric acid **1a** (Table 1, entries 1 and 2). The reaction of dibenzyl azodicarboxylate (**3a**) gave no Diels–Alder product at –20 °C in 1,2-dichloroethane (entry 1).¹¹ On the other hand, the reaction of 2-azopyridinecarboxylate (**3b**),¹² which contained a relatively basic pyridine nitrogen when compared with the carbonyl oxygen of the Cbz group, gave rise to products **5** and **6** (entry 2).^{13,14} Although the reaction of **3b** was not fruitful with regard to yield and regioselectivity, the observed ee of both regioisomers were quite high.¹⁵ To confirm the role of the pyridine nitrogen,^{12b,16} the reaction of 2-azophenylcarboxylate was attempted, and no product was observed under the same conditions. These experiments reveal that the hydrogen bond

Table 1. Catalytic Enantioselective Hetero-Diels–Alder Reaction of 2-Azocarboxylate with Amidodienes^a



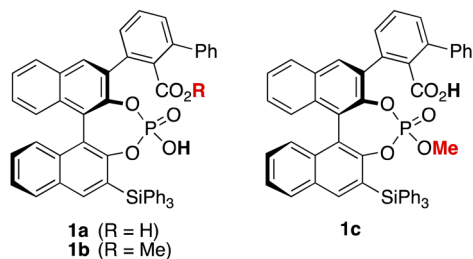
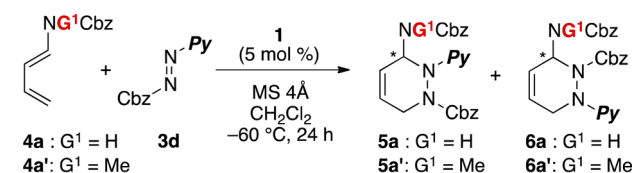
entry	catalyst	3	yield (%) ^b	5:6 ^c	ee (%) ^d	
					5	6
1	1a	3a	<1	–	–	–
2	1a	3b	41	2.4:1	79	74
3	1a	3c	61	>9:1	88	–
4	1a	3d	52	>99:1	97	–
5 ^e	1a	3d	89	>99:1	99	–
6 ^f	none	3d	49	1:2	–	–
7 ^g	2	3d	25	1.9:1	32	29

^aReactions were conducted with 1.0 equiv of **3** and 1.0 equiv of **4a** in the presence of 10 mol % catalyst in 1,2-dichloroethane at –20 °C for 48 h. ^bIsolated yield. ^cDetermined by ¹H NMR. ^dDetermined by chiral HPLC. ^eReaction was conducted with 1.0 equiv of **3** and 2.0 equiv of **4a** in the presence of MS 4 Å and 5 mol % **1a** in dichloromethane at –60 °C for 24 h. ^fReaction was conducted at room temperature for 12 h. ^gReaction was conducted with 1.0 equiv of **3** and 2.0 equiv of **4a** in CH₂Cl₂ at –40 °C.

acceptor such as pyridine nitrogen is the requirement in the **1a**-catalyzed azo-hetero-Diels–Alder reaction.

To improve the stereoselectivity in the system of 2-azopyridinecarboxylate, substitution at the 6-position of the 2-azopyridine was explored; a substituent at the vicinal position of pyridine nitrogen was expected to favorably influence the chiral environment of the transition state (entries 3 and 4). Fascinatingly, improvements in both the regio- and enantioselectivities were indeed realized with the reaction of **3c** and **3d**. The best result was obtained with the reaction of 6-trifluoromethyl-2-azopyridinecarboxylate (**3d**), providing product **5a** with 97% ee as a single regioisomer (entry 4). Finally, high yields and complete regio- and enantioselectivities were achieved under the optimized reaction conditions; i.e., 2 equiv of **4a** and 1 equiv of **3d** were stirred in the presence of molecular sieves 4 Å and 5 mol % **1a** at –60 °C (entry 5). For comparison, the reaction in the absence of catalyst yielded not only **5a** but also a considerable amount of **6a** (entry 6). Finally, when the reaction was conducted in the presence of chiral monophosphoric acid **2**, the yield and stereoselectivity decreased significantly (entry 7).¹⁷ These observations clearly indicate the significant effects of carboxylic acid–cyclic monophosphoric acid **1a** in this transformation.

To gain further insight into the importance of the phosphoric acid and carboxylic acid groups of the catalyst, as well as the *N*-H proton of the amidodiene, we conducted experiments varying these functional groups (Table 2). Methylcarboxylate–phosphoric acid **1b** and carboxylic acid–phosphoric acid

Table 2. Control Experiments^a

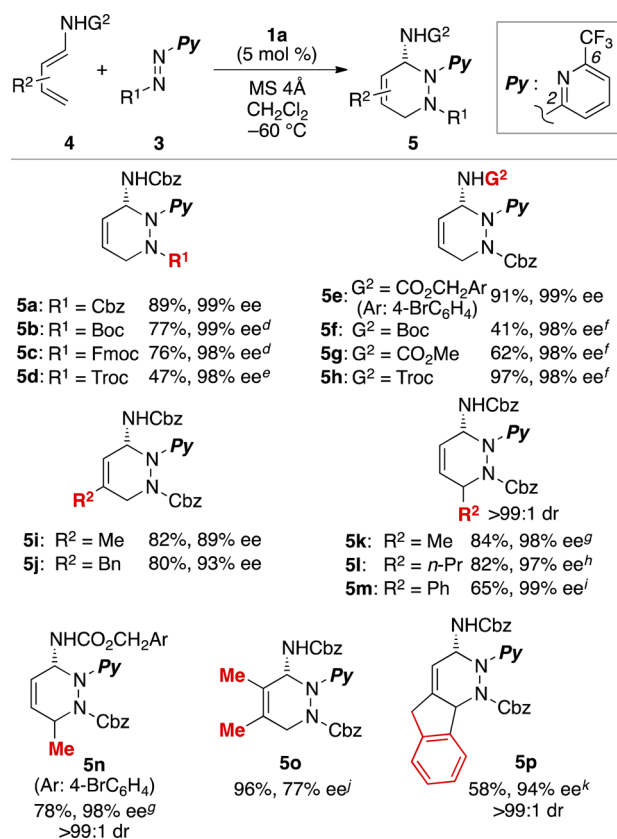
entry	1	G ¹	yield (%) ^b	5:6 ^c	ee (%) ^d	
					5	6
1	1a	H	89	>99:1	99	–
2	1b	H	29	2.2:1	6	11
3	1c	H	<1	–	–	–
4	1a	Me	10	>99:1	36	–

^aReactions were conducted with 1.0 equiv of 3d and 2.0 equiv of 4a in the presence of 5 mol % catalyst and MS 4 Å in CH₂Cl₂ at –60 °C for 24 h. ^bIsolated yield. ^cDetermined by ¹H NMR. ^dDetermined by chiral HPLC.

methyl ester 1c were synthesized, and the reactions of 3d with 4a were examined in the presence of these catalysts (entries 1 and 2). We confirmed that the carboxylic acid moiety significantly affected the reactivity and selectivity of the present azo-hetero-Diels–Alder reaction; replacement of the carboxylic acid with a methylcarboxylate considerably decreased not only the yield but also the regio- and enantioselectivities (entry 1 vs 2, compare also with entry 7 of Table 1). Moreover, methyl phosphate 1c was unable to catalyze the reaction under the same conditions (entry 3). We also found that the reaction with *N*-Me-amidodiene 4a' gave excellent regioselectivities, albeit with extremely poor catalytic and chiral efficiency (entry 4).¹⁸ These results strongly imply that the phosphoric acid–carboxylic acid moieties, the 6-trifluoromethylpyridine substituent, and the N–H of the amidodienes are required to facilitate both the selectivity and reactivity of the reaction. We presume the intra- and intermolecular hydrogen-bonding interactions among these contribute to creating the chiral environment to produce the excellent regio-, diastereo-, and enantioselectivity of this reaction.

The scope of the azo-hetero-Diels–Alder reaction was investigated (Chart 1). High enantiomeric excess was observed with 5a–5h regardless of the acyloxy group on both 2-azopyridines 3 and amidodienes 4. Moreover, a variety of 3- and 4-substituted amidodienes were applicable to give 5i–5n in good yields, with high enantioselectivities. In the cases of 4-substituted compounds, the products 5k–5n were obtained as single diastereomers. When 2,3-disubstituted amidodiene was used, the enantiomeric excess of 5o dropped significantly. In contrast, 3,4-disubstituted amidodiene gave 5p in high enantiomeric excess, but the yield was moderate.

2. Computational Study by Density Functional Theory (DFT) Calculations. To explore the hydrogen-bonding network in the present catalysis, theoretical investigations of the detailed transition state (TS) models were conducted on

Chart 1. Reaction Scope^{a,b,c}

^aReactions were conducted with 1.0 equiv of 3 and 2.0 equiv of 4 in the presence of 5 mol % catalyst and MS 4 Å in CH₂Cl₂ at –60 °C for 24 h. ^bIsolated yield. ^cDetermined by chiral HPLC. ^d45 h. ^e55 h. ^f40 h. ^g–40 °C, 48 h. ^h–40 °C, 72 h. ⁱ10 mol %, –20 °C, 72 h. ^j–60 °C, 72 h. ^k10 mol %, –40 °C, 48 h.

the 1a-catalyzed reaction of 3d with 4a using density functional theory (DFT) calculations.¹⁹ Regarding the axial chirality of the phenyl–naphthyl axis in 1a, both DFT calculations and X-ray diffraction analysis showed the (*S*)-configuration is more stable than the (*R*)-configuration due to the intervention of hydrogen bond between carboxylic acid and monophosphoric acid.²⁰ The control experiments shown in Table 2 suggest that the phosphoric acid moiety is needed to promote the present azo-hetero-Diels–Alder reaction and the carboxylic acid moiety plays an important role in achieving the high chemical yields and selectivities. Under this hypothesis, we focused on TS models in which 3d and 4a are activated by the phosphoric acid moiety of 1a. Based on the previously reported theoretical study of the bis-phosphoric acid catalysis,^{6b} various coordination models were explored (Figure 3a). There are two possibilities of the carboxylic acid-bridged 1a structures: 1a-model A and 1a-model B. In spite of the thermodynamic stability of 1a-model B, the most energetically favored TS structures include 1a-model A (see Supporting Information). This is due to the enhancement of the acidity^{6,21} while keeping the basicity in the phosphoric acid and phosphoryl oxygen residues, both which induce the strong interaction with 3d and 4a. Regarding diastereomeric TSs derived from 1a-model A corresponding to the enantiofacial selection of 4a (leading to (*R*) and (*S*) enantiomers of 5a, TS_r, and TS_s), the relative orientation of 3d (TS_{endo}, TS_{exo}), and three coordination modes (TS1: N¹, H⁰; TS2: O², H⁰; TS3: N³, H⁰) were

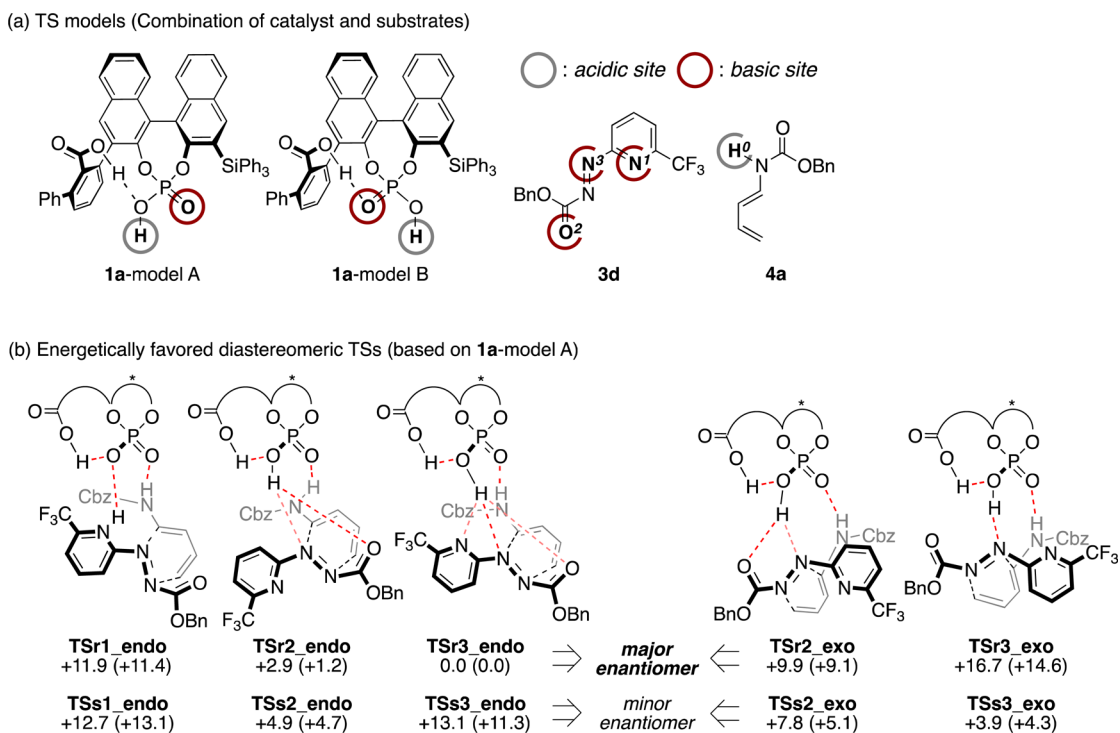


Figure 3. (a) Coordination models of diastereomeric TSs and (b) the relative energy differences of energetically favored diastereomeric TSs. Coordination modes: **TS1** (N^1, H^0), **TS2** (O^2, H^0), **TS3** (N^3, H^0).

compared (Figure 3b; see Supporting Information).²² **TSr3_endo** leads to the major (*R*)-enantiomer and is energetically most favored of all of the diastereomeric TSs. For TSs leading to the minor (*S*)-enantiomer, **TSs2_endo** and **TSs3_exo** are located at a similar energy level, albeit 4.9 and 3.9 kcal/mol less stable, respectively, than the most stable **TSr3_endo**. These computational results are qualitatively consistent with the experimental results. In the energetically disfavored **TS1_endo**, pyridinium phosphate is formed through the proton transfer from the phosphoric acid moiety.²³

To reveal the origin of the high enantioselectivity, the notable structural features of the relatively stable **TSr3_endo**, **TSs2_endo**, and **TSs3_exo** were investigated in detail (Figure 4). Both **3d** and **4a** fit well in the chiral space of **1a** constructed by the intramolecular hydrogen bond between two acidic functional groups in **TSr3_endo**. As predicted in our catalyst design discussed with Figure 2, there exist multiple secondary interactions—weak intermolecular hydrogen bonds—between **3d** and **1a** in **TSr3_endo**. Furthermore, the nonclassical CH/O hydrogen bonds are formed between the benzene ring (Cbz) of **3d** and the carboxylic moiety of **1a**. The lack of significant steric stress and the formation of the effective hydrogen-bonding network stabilize **TSr3_endo** (Figure 4a). In contrast, **TSs2_endo**, leading to the minor enantiomer, has unfavorable steric interactions between two aryl groups (Cbz and 6-trifluoromethylpyridine) of **3d** and the sterically demanding $SiPh_3$ group of **1a**. Such steric repulsions result in the lack of the hydrogen-bonding network between **3d** and **1a**, destabilizing **TSs2_endo** (Figure 4b). In a manner similar to **TSr3_endo**, both **3d** and **4a** are well oriented in the chiral space of **1a** in **TSs3_exo** without any unfavorable steric interactions with **1a**. As for **4a**, however, the C–N bond rotation leading to the facial selectivity inversion of **4a** (i.e., leading to minor enantiomer) induces the strong steric

repulsion between the *N*-Cbz group and the diene moiety. This is responsible for destabilization of **TSs3_exo** (Figure 4c).

To identify the main factor in determining the relative energy difference among **TSr3_endo**, **TSs2_endo**, and **TSs3_exo**, a distortion/interaction analysis²⁴ was carried out (Table 3). The interaction energy difference between **1a** and **3d/4a** ($\Delta INT = +11.2$ kcal/mol) has a larger impact on destabilization of **TSs2_endo** than other factors. On the other hand, the distortion energy difference of **3d/4a** ($\Delta DEF_{sub} = +4.8$ kcal/mol), mainly derived from the steric interaction between the *N*-Cbz group and the diene moiety, exerts a significant influence in the stability of **TSs3_exo**. This is attributed to destabilization of **TSs3_exo**. These structural and distortion/interaction analyses indicate the elaborated chiral space and the effective hydrogen-bonding network derived from the two acidic functionalities in **1a** that synergistically control the stereoselectivity of **5**.

CONCLUSIONS

We have developed a chiral Brønsted acid with two different acidic sites, carboxylic acid–monophosphoric acid **1a**, and this novel catalyst structure has proven to be a highly effective catalyst for asymmetric hetero-Diels–Alder reactions between 6-trifluoromethyl-2-azopyridinecarboxylates and *N*-*H*-amidodienes. The reactions proceed in good yields and excellent regio-, diastereo-, and enantioselectivities with a wide range of substituent patterns. A mechanistic study by DFT calculations revealed that the multipoint hydrogen-bonding interactions among the carboxylic acid, monophosphoric acid, 2-azopyridinecarboxylate, and *N*-*H*-amidodiene moieties are key in this catalysis. The two Brønsted acidic sites, the carboxylic acid and monophosphoric acid groups, cooperatively function to result in high catalytic and chiral efficiencies. The present work represents the first successful design of a combined carboxylic

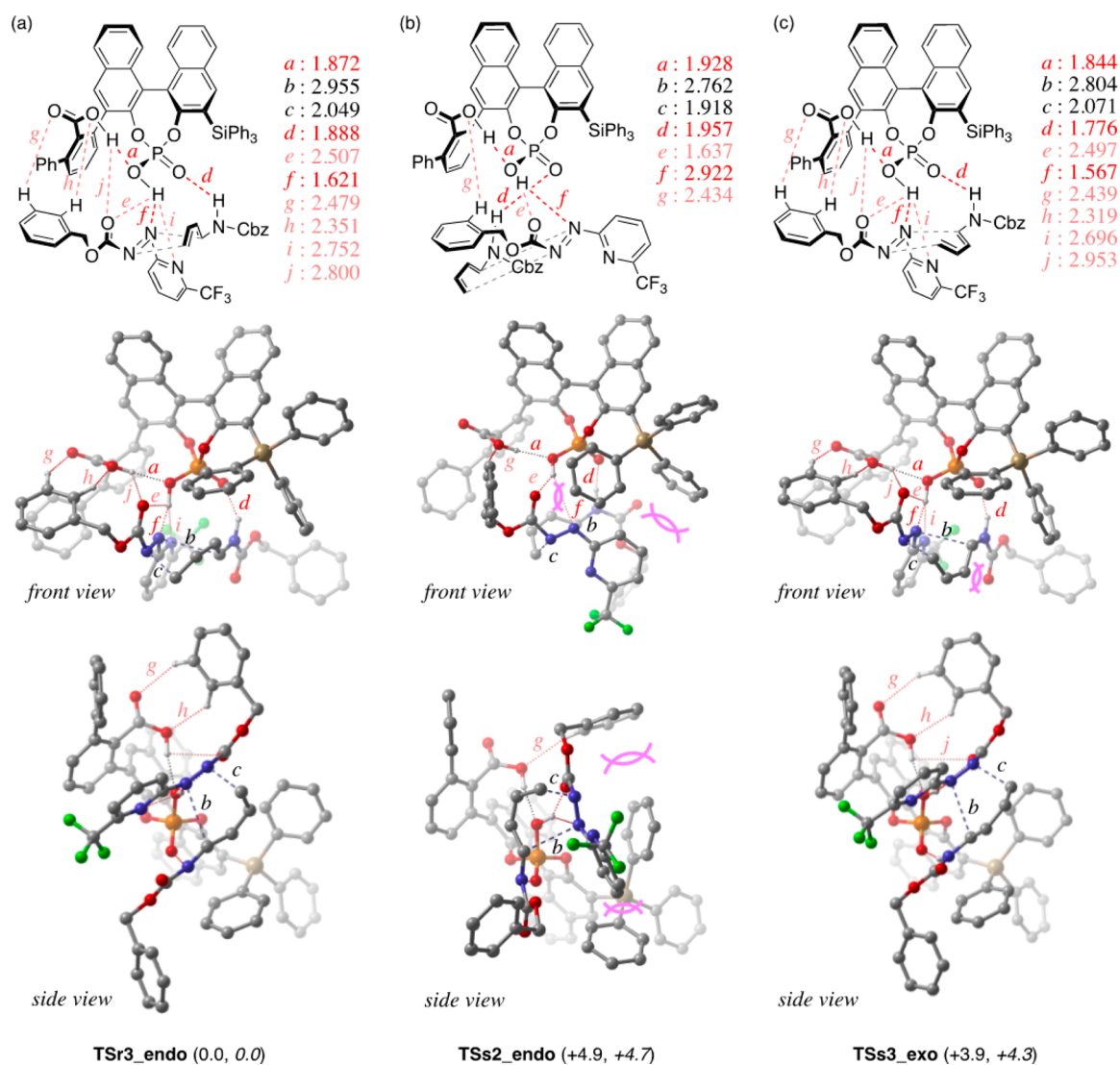


Figure 4. Length of hydrogen bonds, front and side views of 3D structures, the relative energies (in plain, kcal/mol), and the relative Gibbs free energies (in *italics*, kcal/mol) of (a) TSr3_endo, (b) TSs2_endo, and (c) TSs3_exo.

Table 3. Distortion/Interaction Analysis of TSr3_endo, TSs2_endo, and TSs3_exo (kcal/mol)

entry	TS	$\Delta\text{DEF}_{\text{cat}}^a$	$\Delta\text{DEF}_{\text{sub}}^a$	ΔINT^b
1	TSr3_endo	0	0	0
2	TSs2_endo	-6.4	+0.1	+11.2
3	TSs3_exo	+1.5	+4.8	-2.4

^a $\Delta\text{DEF} = \text{DEF}(\text{TS}) - \text{DEF}(\text{TSr3_endo})$. ^b $\Delta\text{INT} = \text{INT}(\text{TS}) - \text{INT}(\text{TSr3_endo})$.

acid–phosphoric acid in chiral Brønsted acid catalysis, and further studies on chiral Brønsted acids with different acidic sites are underway in our laboratories and will be reported in due course.

■ ASSOCIATED CONTENT

📄 Supporting Information

The Supporting Information is available free of charge on the ACS Publications website at DOI: 10.1021/jacs.6b07150.

Experimental details, characterization data, HPLC enantiomer analysis, NMR spectra for new compounds, X-ray diffraction analysis, and Cartesian coordinates (PDF)

Crystallographic data for **1a** and regioisomers **5e/6** (CIF, CIF, CIF)

■ AUTHOR INFORMATION

Corresponding Authors

*momiyama@ims.ac.jp
*mterada@m.tohoku.ac.jp

Notes

The authors declare no competing financial interest.

ACKNOWLEDGMENTS

Support was partially provided by IMS, JSPS via Grant-in-Aid for Scientific Research C (No. 23550114) for N.M., and Grant-in-Aid for Scientific Research on Innovative Area “Advanced Molecular Transformations by Organocatalysts” from MEXT, Japan (No. 23105002 for M.T., No. 23105005 for M.Y.). We sincerely thank Dr. Koji Yamamoto, Research Center of Integrative Molecular System, Institute for Molecular Science for the X-ray crystallographic analysis of **5e**, and Fuji Silysia Chemical Ltd. for the gift of CHROMATOREX-DIOL. N.M., T.F., and K.Y. gratefully acknowledge JST-ACCEL for financial support. H.T. acknowledges JSPS for a Research Fellowship for Young Scientists. K.F. thanks the Yoshida Scholarship Foundation.

REFERENCES

- (1) For selected reviews of chiral Brønsted acid catalysts, see: (a) Akiyama, T.; Itoh, J.; Fuchibe, K. *Adv. Synth. Catal.* **2006**, *348*, 999–1010. (b) Kampen, D.; Reisinger, C. M.; List, B. *Top. Curr. Chem.* **2009**, *291*, 395–456. (c) Trkmen, Y. E.; Zhu, Y.; Rawal, V. H. In *Comprehensive Enantioselective Organocatalysis*; Dalko, P. I., Ed.; Wiley: Weinheim, 2013; Vol. 2, pp 241–288. (d) Akiyama, T.; Mori, K. *Chem. Rev.* **2015**, *115*, 9277–9306.
- (2) For references of each chiral Brønsted acid catalyst, see the [Supporting Information](#).
- (3) (a) Momiyama, N.; Yamamoto, H. *J. Am. Chem. Soc.* **2005**, *127*, 1080–1081. (b) Hasegawa, A.; Naganawa, Y.; Fushimi, M.; Ishihara, K.; Yamamoto, H. *Org. Lett.* **2006**, *8*, 3175–3178. (c) Jones, C. R.; Dan Pantos, G. D.; Morrison, A. J.; Smith, M. D. *Angew. Chem., Int. Ed.* **2009**, *48*, 7391–7394. (d) Probst, N.; Madarasz, A.; Valkonen, A.; Papai, I.; Rissanen, K.; Neuvonen, A.; Pihko, P. M. *Angew. Chem., Int. Ed.* **2012**, *51*, 8495–8499. (e) Min, C.; Mittal, N.; Sun, D. X.; Seidel, D. *Angew. Chem., Int. Ed.* **2013**, *52*, 14084–14088. (f) Ratjen, L.; van Gemmeren, M.; Pesciaoli, F.; List, B. *Angew. Chem., Int. Ed.* **2014**, *53*, 8765–8769. (g) Min, C.; Lin, C.-T.; Seidel, D. *Angew. Chem., Int. Ed.* **2015**, *54*, 6608–6612.
- (4) For representative reviews of chiral phosphoric acid, see: (a) Terada, M. *Synthesis* **2010**, *2010*, 1929–1982. (b) Akiyama, T. In *Asymmetric Synthesis II*; Christmann, M., Brase, S., Eds.; Wiley-VCH: Weinheim, 2012; pp 261–266. (c) Parmar, D.; Sugiono, E.; Raja, S.; Rueping, M. *Chem. Rev.* **2014**, *114*, 9047–9153.
- (5) Momiyama, N.; Narumi, T.; Terada, M. *Chem. Commun.* **2015**, *51*, 16976–16979.
- (6) (a) Momiyama, N.; Konno, T.; Furiya, Y.; Iwamoto, T.; Terada, M. *J. Am. Chem. Soc.* **2011**, *133*, 19294–19297. (b) Momiyama, N.; Funayama, K.; Noda, H.; Yamanaka, M.; Akasaka, N.; Ishida, S.; Iwamoto, T.; Terada, M. *ACS Catal.* **2016**, *6*, 949–956.
- (7) For representative reviews of multipoint control by chiral metal catalyst, see: (a) Matsunaga, S.; Shibasaki, M. *Synthesis* **2013**, *45*, 421–437. (b) Matsunaga, S.; Shibasaki, M. *Chem. Commun.* **2014**, *50*, 1044–1057.
- (8) For representative reviews of asymmetric hetero-Diels–Alder reaction, see: (a) Jørgensen, K. A. *Angew. Chem., Int. Ed.* **2000**, *39*, 3558–3588. (b) Jørgensen, K. A. *Eur. J. Org. Chem.* **2004**, *2004*, 2093–2102. (c) Lin, L.; Liu, X.; Feng, X. *Synlett* **2007**, *2007*, 2147–2157. (d) Pellissier, H. *Tetrahedron* **2009**, *65*, 2839–2877. (e) Masson, G.; Lalli, C.; Benohoud, M.; Dagoussat, G. *Chem. Soc. Rev.* **2013**, *42*, 902–923. (f) Du, H.; Ding, K. In *Comprehensive Enantioselective Organocatalysis: Catalysts, Reactions, and Applications*; Kalko, P. I., Ed.; Wiley-VCH Verlag GmbH & Co. KGaA: Weinheim, 2013; Vol. 3, pp 1131–1162. (g) Ishihara, K.; Sakakura, A. In *Comprehensive Organic Synthesis*, 2nd ed.; Knochel, P., Molander, G. A., Eds.; Elsevier: Oxford, 2014; Vol. 5, pp 409–465.
- (9) For representative examples of enantioselective azo-hetero-Diels–Alder reactions, see: (a) Aburel, P. S.; Zhuang, W.; Hazell, R. G.; Jørgensen, K. A. *Org. Biomol. Chem.* **2005**, *3*, 2344–2349. (b) Liu, B.; Li, K.-N.; Luo, S.-W.; Huang, J.-Z.; Huan, P.; Gong, L.-Z. *J. Am. Chem. Soc.* **2013**, *135*, 3323–3326. (c) Liu, B.; Liu, T.-Y.; Luo, S.-W.; Gong, L.-Z. *Org. Lett.* **2014**, *16*, 6164–6167.
- (10) For reviews of enantioselective aza-Diels–Alder reaction, see: (a) Yamamoto, H.; Kawasaki, M. *Bull. Chem. Soc. Jpn.* **2007**, *80*, 595–607. (b) Ukaji, Y. In *Comprehensive Chirality*; Carreira, E. M., Yamamoto, H., Eds.; Elsevier: Oxford, 2012; Vol. 5, pp 470–501.
- (11) Amidodiene **4a** decomposed during the reaction.
- (12) (a) Srinivasan, V.; Jebaratnam, D. J.; Budil, D. E. *J. Org. Chem.* **1999**, *64*, 5644–5649. (b) Kawasaki, M.; Yamamoto, H. *J. Am. Chem. Soc.* **2006**, *128*, 16482–16483.
- (13) (a) Nakamura, S.; Nakashima, H.; Yamamura, A.; Shibata, N.; Toru, T. *Adv. Synth. Catal.* **2008**, *350*, 1209–1212. (b) Nakamura, S.; Sakurai, Y.; Nakashima, H.; Shibata, N.; Toru, T. *Synlett* **2009**, *2009*, 1639–1642. (c) Nakamura, S.; Maeno, Y.; Ohara, M.; Yamamura, A.; Funahashi, Y.; Shibata, N. *Org. Lett.* **2012**, *14*, 2960–2963.
- (14) For X-ray crystallographic analyses of Brønsted acid–pyridine complexes, see: (a) Panneerselvam, K.; Hansongnern, K.; Rattanawit, N.; Liao, F.-L.; Lu, T.-H. *Anal. Sci.* **2000**, *16*, 1107–1108. (b) Hashimoto, T.; Kimura, H.; Nakatsu, H.; Maruoka, K. *J. Org. Chem.* **2011**, *76*, 6030–6037.
- (15) For absolute configuration of each regioisomer was determined by X-ray diffraction analysis; see [Supporting Information](#).
- (16) (a) Yin, L.; Brewitz, L.; Kumagai, N.; Shibasaki, M. *J. Am. Chem. Soc.* **2014**, *136*, 17958–17961. (b) Brewitz, L.; Arteaga, F. A.; Yin, L.; Alagiri, K.; Kumagai, N.; Shibasaki, M. *J. Am. Chem. Soc.* **2015**, *137*, 15929–15939.
- (17) The reactions were also attempted in the presence of 10 mol % chiral monophosphoric acids with 2,4,6-triisopropylphenyl or bis-trifluoromethylphenyl group. The desired azo-hetero-Diels–Alder products were obtained; however, chemical yields and selectivities were less than those by **1a**. In the presence of monophosphoric acid with a 2,4,6-triisopropylphenyl group: 58% yield, **5a:6a** = 19:1, 99% ee of **5a**. In the presence of monophosphoric acid with 3,5-bis-trifluoromethylphenyl group: 13% yield, **5a:6a** = 1.3:1, 90% ee of **5a**, 84% ee of **6a**.
- (18) The reaction of **3d** with 1-methoxybuta-1,3-diene was also attempted in the presence of 10 mol % **1a**. The reaction gave the product at 0 °C for 20 h; however, the yield and selectivities were insufficient (yield of two isomers: 22%, regioisomer ratio: 49/1, ~40% ee for major regioisomer).
- (19) Frisch, M. J.; Trucks, G. W.; Schlegel, H. B.; Scuseria, G. E.; Robb, M. A.; Cheeseman, J. R.; Scalmani, G.; Barone, V.; Mennucci, B.; Petersson, G. A.; Nakatsuji, H.; Caricato, M.; Li, X.; Hratchian, H. P.; Izmaylov, A. F.; Bloino, J.; Zheng, G.; Sonnenberg, J. L.; Hada, M.; Ehara, M.; Toyota, K.; Fukuda, R.; Hasegawa, J.; Ishida, M.; Nakajima, T.; Honda, Y.; Kitao, O.; Nakai, H.; Vreven, T.; Montgomery, J. A., Jr.; Peralta, J. E.; Ogliaro, F.; Bearpark, M.; Heyd, J. J.; Brothers, E.; Kudin, K. N.; Staroverov, V. N.; Keith, T.; Kobayashi, R.; Normand, J.; Raghavachari, K.; Rendell, A.; Burant, J. C.; Iyengar, S. S.; Tomasi, J.; Cossi, M.; Rega, N.; Millam, J. M.; Klene, M.; Knox, J. E.; Cross, J. B.; Bakken, V.; Adamo, C.; Jaramillo, J.; Gomperts, R.; Stratmann, R. E.; Yazyev, O.; Austin, A. J.; Cammi, R.; Pomelli, C.; Ochterski, J. W.; Martin, R. L.; Morokuma, K.; Zakrzewski, V. G.; Voth, G. A.; Salvador, P.; Dannenberg, J. J.; Dapprich, S.; Daniels, A. D.; Farkas, O.; Foresman, J. B.; Ortiz, J. V.; Cioslowski, J.; Fox, D. *Gaussian 09*, Revision D.01; Gaussian, Inc.: Wallingford, CT, 2013. Details of DFT calculations are shown in the [Supporting Information](#).
- (20) For details for X-ray diffraction analysis of **1a**, see: [Supporting Information](#).
- (21) He, L.; Chen, X. H.; Wang, D.; Luo, S. W.; Zhang, W. Q.; Yu, J.; Ren, L.; Gong, L. Z. *J. Am. Chem. Soc.* **2011**, *133*, 13504–13518.
- (22) Both **TSr1_exo** and **TSs1_exo** were unable to be optimized by structural and geometric restrictions.
- (23) Yamanaka, M.; Itoh, J.; Fuchibe, K.; Akiyama, T. *J. Am. Chem. Soc.* **2007**, *129*, 6756–6764.

(24) The energies of TS were dissected into the distortion (DEF) and interaction energies (INT) for the two distorted fragments (**1a** and **3d/4a**) constructing TS. The differences for each energies (DDEF and DINT) among diastereomeric TSs were calculated by the counterpoise method. For the original distortion/interaction analysis, see: (a) Morokuma, K.; Kitaura, K. In *Chemical Applications of Atomic and Molecular Electrostatic Potentials*; Politzer, P., Truhlar, D. G., Eds.; Plenum: New York, 1981; pp 215–242. (b) Ess, D. H.; Houk, K. N. *J. Am. Chem. Soc.* **2007**, *129*, 10646–10647. (c) Ess, D. H.; Houk, K. N. *J. Am. Chem. Soc.* **2008**, *130*, 10187–10198. (d) Lam, Y.-H.; Cheong, P. H.-Y.; Blasco Mata, J. M.; Stanway, S. J.; Gouverneur, V.; Houk, K. N. *J. Am. Chem. Soc.* **2009**, *131*, 1947–1957. (e) Paton, R. S.; Kim, S.; Ross, A. G.; Danishefsky, S. J.; Houk, K. N. *Angew. Chem., Int. Ed.* **2011**, *50*, 10366–10368. (f) Green, A. G.; Liu, P.; Merlic, C. A.; Houk, K. N. *J. Am. Chem. Soc.* **2014**, *136*, 4575–4583.